STUDIES OF BASIC ELECTRONIC PROPERTIES OF CdTe-BASED SOLAR CELLS & THEIR EVOLUTION DURING PROCESSING & STRESS

Quarterly Technical Status Report for the Quarter ended July 31, 2003

Under Prime Contract No. DE-AC36-99-GO1033
Subcontract No. ADJ-2-30630-05

Subcontractor: Colorado School of Mines

Principal Investigators: V. Kaydanov and T. R. Ohno

Contributors:

Professors Reuben T. Collins and Colin A. Wolden

Grad. Research Associates J. Kestner, S. Kelly, and S. Feldman

Contract technical monitor: Kenneth Zweibel

During the quarter from May 2003 to July 31, 2003 we introduced new instrumentation for acquisition of high spatial-resolution imaging electroluminescence (EL) with spectroscopic measurements on the same length scale. This was intended to complement our existing system based on a Santa Barbara Instrument Group ST-5C CCD camera with microsope objectives that provided higher spatial resolution (diffraction limited to ~ 1μm) but measured only the integrated EL intensity. Results are presented for samples that have intentional non-uniformity due to back contact preparation. We also completed analysis of the newly-named Gas Jet Deposition system (GJD), previously called Jet Vapor Deposition (JVD). Emphasis was on modeling to understanding the role of different processing parameters on CdTe growth rate. In addition a first attempt was made at re-examination of incorporation of buffer layers in CdTe-based cells using GJD.

EL measurements

Lateral spatial non-uniformities in cells has been proposed as a cause of observed variability in the efficiency and stability of cells and modules [1]. In previous reports we presented room temperature, integrated EL maps of both as-prepared and stressed sample cells. The material was from many growth methods and post-growth processing steps. In the images there were a number of commonly observed features:

1. On all length scales measured there were spatial variations in the integrated EL emission indicating non-uniformities. For one particular set we quantified this with variogram analysis for a small fragment of a cell EL image. Correlations at separations of 10 and 60 μm were observed, however larger lengths may be observed on larger samples.
2. Occasionally a "ring" was observed on the contact perimeter that has been associated with current collection in the material beyond the contact [team meet]. We were able to confirm this interpretation on a sample by scribing an interior region, which then showed no edge enhancement in the absence of uncontacted CdTe.

3. Intensity for stressed samples usually decreased relative to the same cells before stress. The nature of the stress (duration, bias) affected how the pattern of the emission changed.

Histograms of the intensity in each pixel can be used to represent the distribution graphically. However for ease of comparison a few numerical figures of merit are used. The integrated average intensity per pixel, which depends on the excitation current, magnification and measurement time as well as the cell properties, can be used to compare images acquired under the same conditions. We defined the non-uniformity as the standard deviation divided by the average integrated intensity. The following tables summarize results for unstressed and stressed samples. Table 1 lists values from samples measured as part of the Non-Uniformity subteam, with some images presented in the Phase I Annual report.

Cell	Stressed?	Eff	Jsc	Voc	FF	EL Mean	EL St Dev.	Nonuniformity
CSU No Cu	no	4.5	15.3	0.66	44	631	94	0.126
CSU 0.5 min Cu	no	9.7	18.9	0.75	68	3417	465	0.132
CSU 1 min Cu	no	9.7	18.5	0.75	70	2649	322	0.115
CSU 4 min Cu	no	9.3	19.8	0.75	62	2547	265	0.097
CSU No Cu	yes	0.8	6.52	0.59	20	622	76	0.092
CSU 0.5 min Cu	yes	5.9	19.5	0.74	41	3153	505	0.156
CSU 1 min Cu	yes	7.9	19.1	0.74	55	3483	644	0.188
CSU 4 min Cu	yes	10	20.1	0.74	70	2005	343	0.166
FS w/UT contact	no	10	19.2	0.8	67	18150	2856	0.159
FS w/UT contact	yes	8.2	17	0.77	62	5844	1190	0.211
UT sputtered	no	3	17.8	0.56	30	16814	2856	0.157
UT sputtered	yes	4.7	17.3	0.69	39	7974	1190	0.204

Table 1 Integrated EL intensity measured with injected current density J = 600 mA/cm^2. The unstressed UT sample showed some contact damage. Stress conditions were 4 weeks at 65^{o}C, light, open circuit.

The most notable difference between cells prepared with different growth methods was the lower mean intensity of the CSU grown material, as noted previously. In addition stress usually resulted in the reduction in EL mean intensity by about 3, while this was not the case for the CSU material. A less certain conclusion for these moderately stressed samples was a small but apparent increase in non-uniformity.

In order to further study this effect, a more severely-stressed set was used in the second investigation for the Non-Uniformity subteam. Unstressed images were reported in the January 2003 quarterly and stressed images were presented at the Summer 2003 CdTe team meeting. The table below lists figures of merit for the normal cell performance parameters and EL. This set again shows reductions in mean EL emission with stress, ranging from 2 to 7 times (no CSU cells were measured in this set, and those tested started with similar initial values).

Cell	Stressed?	Eff	Jsc	Voc	FF	EL Mean	EL St Dev.	Nonuniformity
FS17	no	10.72	19.74	0.83	65.74	1027	210	0.227
FS17	yes	5.43	15.9	0.64	57.6	133	104	3.39
FS16	no	9.07	17.37	0.83	63.24	1177	238	0.221
FS16	yes	5.19	13.6	0.66	53	135	185	5.43
USF9	no	18.35	37.09	0.84	59.21	1084	279	0.280
USF9	yes	11.96	29.4	0.75	51.9	260	72	0.452
USF11	no	12.13	35.9	0.84	40.44	805	107	0.154
USF11	yes	9.89	25.1	0.75	50.1	415	91	0.289
UT20	no	12.8	23.39	0.83	65.67	942	98	0.112
UT20	yes	0.39	15.1	0.1	24.7	227	46	0.368
UT26	no	11.1	22.39	0.83	59.43	972	94	0.108
UT26	yes	8.05	17.7	0.75	60.7	187	75	0.863

Table 2 **Integrated EL intensity measured with injection current density J ~ 33 mA/cm^2. Current density for USF cells are less certain due to ragged area. Stressed UT20 had a damaged contact, but was included for completeness.**

Now we are able to more conclusively state that non-uniformity increased with stress, with changes that range from 2 to 15 times. Comparison with similar (but not the same) samples measured with other spatially-resolved techniques such as photoluminescence (PL) at the University of Toledo or photocurrent mapping at CSU did not show clear correlations. Thermography matched better, showing a 3x increase in mean value and increased non-uniformity with stress, as well as occasional 'rings' on the contact edge [2]. Higher temperatures for stressed cells with lower EL emission seems reasonable, as more non-radiative recombination may have occurred. This suggests that both EL and thermography non-uniformity reflects localization of current flow.

The most pronounced change in non-uniformity was for the First Solar samples. The I-V dark curves provide evidence of dramatic change in the cell. Figure 1 shows increased rollover, suggesting an increased series resistance, likely due to a back contact diode. While normally attributed to uniform change in a one-dimensional model we will show that this may be related to non-uniformity as well.

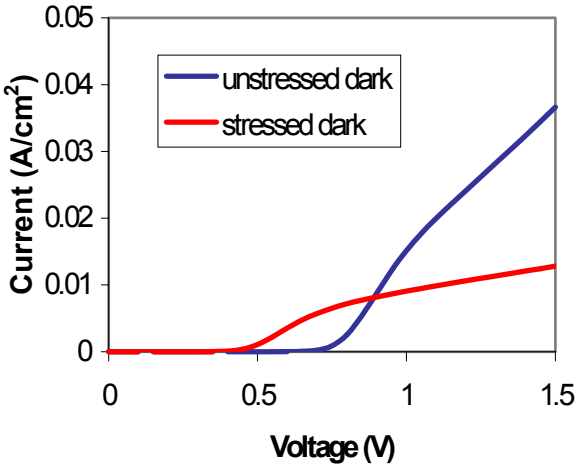

Figure 1 First Solar sample from Table 2 show lumped results of stressing.

In conclusion the previous results suggest that EL emission can be related to changes in stressed cells. However there remain important unresolved questions. The natures of the electronic states involved in EL are not known since we observe only the integrated EL intensity. This is in contrast to PL studies by Grecu et al. [3] that allow association of peaks in the PL spectra with defects due to different procedures. Another question is whether the observed variation is due to changes in the back contact barrier, the main (CdTe-CdS) junction or some other element in the injected current path. We have reported a small set of controlled process variation experiments with the purpose of determining contributing factors for the non-uniformity. Changes in the amount of copper (Cu) and ZnTe in the primary back contact or the thickness of the Au used in the secondary contact has a large impact on the uniformity and intensity, suggesting back contact barrier effects were dominant. To pursue these questions we installed new equipment with spatially-resolved spectroscopic measurements and manufactured samples with intentionally introduced non-uniformities.

The system used was a Princeton Instruments Spec-10:100BR Digital CCD Spectroscopy System with liquid nitrogen-cooled, back-illuminated, deep-depletion CCD camera (1340 x 100 pixels with 20 x 20μm pixels) The monochromator/spectrograph was capable of operation in a two-dimensional imaging mode or a one-dimensional spatial mode with spectroscopic data. Because of the increased sensitivity of the CCD data can be acquired much more rapidly at lower levels of injection. At higher injection rates deep states are all saturated and cannot be seen as well. The spectrometer optics are such that magnification is limited so the 20 μm pixels place a limit on the spatial resolution of ~ 10 μm. Another feature of the high sensitivity is that we can change the excitation source from injected current to a low powered laser such as a He-Ne laser to perform PL on the same cell that is used for EL measurements. PL and EL are very similar techniques in that they both rely upon the radiative recombination of carriers. They differ, however, in injection method. PL injects carriers relatively uniformly across the illuminated area with an extended laser beam, but only to a few absorption lengths depthwise. From the glass side this is near the CdTe junction. EL injects holes through the back contact, though they mostly recombine in the CdTe near the main junction, since both hole and electron densities must be high. As a result both emissions are from the same region. However, if the back contact barrier is not uniform the current density also is not, resulting in EL spatial variations.

Features of the order of 100 μm are easily observed with this spectrometer and provided an ideal test of the instrument. The simplest way to introduce non-uniformity was deposition of 150 μm diameter Cu dots though a mask. The Cu was then diffused and etched. A comparatively large (~2mm) Au pad was deposited over many Cu dots as per the standard CSM Cu/Au back contact. This cell was compared to a standard cell processed with Cu deposited over the entire back of the CdTe film. The process is graphically illustrated below.

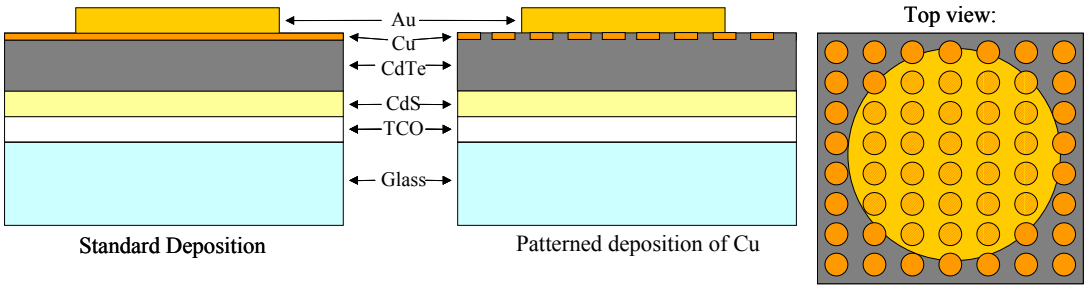

Figure 2 Schematic of patterned deposition to intentionally introduce non-uniformity

Areas with Cu should have a lower back contact barrier than areas without Cu, and current density would be higher than the areas without Cu, show more EL emission. This effect is exactly what is seen in the EL images below.

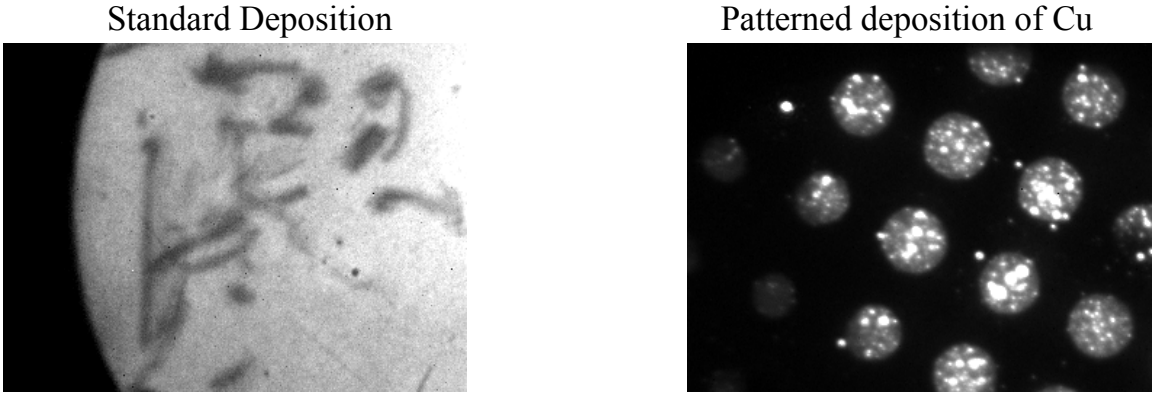

Figure 3 Integrated EL emission for patterned Cu deposition and normal uniform Cu used in standard process, with same average current density. Dark marks in the left image are caused by scratches from contacts. Dim EL emission was seen in areas without intentional Cu, but was ~10x less than the areas with Cu.

Figure 4 shows the effect of the non-uniform back contact barrier on dark I-V curves. The resemblance to Figure 1 suggests that this manufactured sample may be similar to the degraded FS sample. It also illustrates the difficulty in interpretation of I-V curves using one-dimensional modeling.

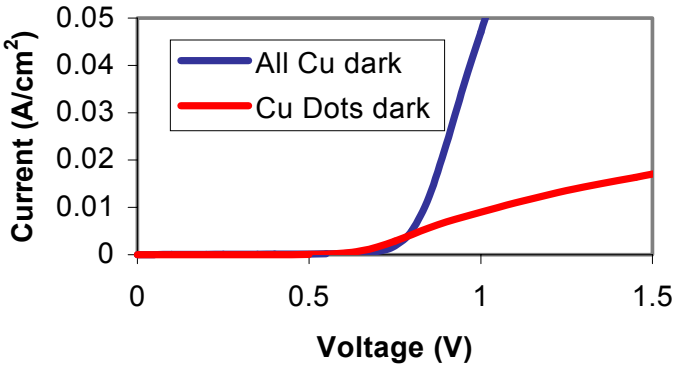

Figure 4 I-V measurements for standard cell and patterned cell in Fig. 3.

Consecutive EL and PL measurements on the same place can distinguish changes in EL due to recombination processes near the main (CdTe-CdS) junction or back contact diode effects. Aligned EL and PL features are probably main junction effects, while structure in EL that does not show up in PL are probably back contact effects. EL and PL measurements were done on the stressed FS cell (Table 2) from the Non-Uniformity subteam as well as on the cell with Cu dots.

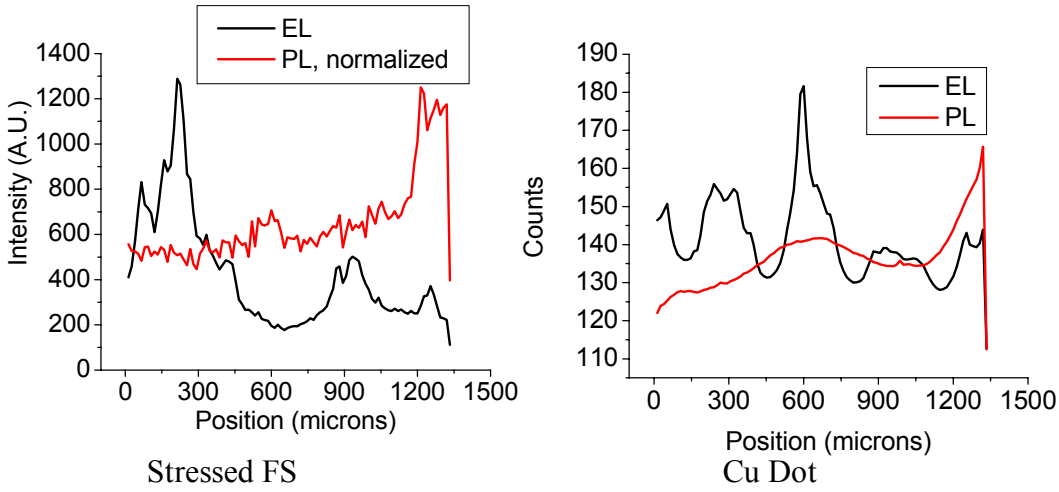

Figure 5 **Line scans of EL and PL intensity. The left graph is from the FS cell and the right graph is from the Cu dot cell.**

Bright features can be seen in the FS cell in EL, but these features do not correspond to PL features. In the patterned Cu dot cell, the repeated pattern of Cu dots can easily be seen in the EL, but though the PL appears to have some structure to it, the structure does not correspond to PL features. This is very indicative of back contact diode effects in both samples.

Spectra were also taken at the same time (Figure 6). The same features are seen in EL and PL, albeit with different relative amplitudes. As a result of low injection rates for both EL and PL transitions associated with deeper levels (sub band gap emission) were most prominent.

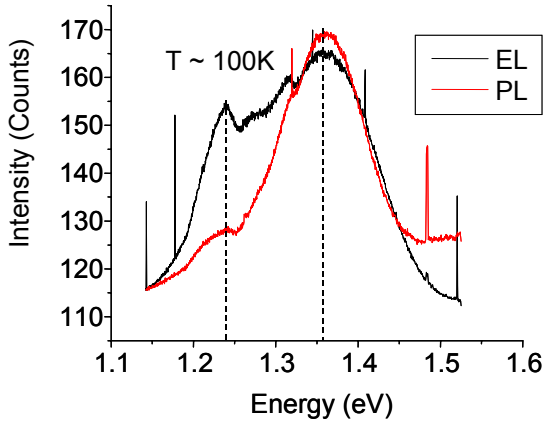

Figure 6 **Luminescence spectra measured on Cu dot sample. PL was excited with He-Ne laser spread by a cylindrical lens. EL excitation was 12 mA/cm^2 and PL was 20 mW/cm^2.**

Simultaneous spectra was acquired at each point of the slit. Spectra at different positions showed variations in relative amplitudes of peaks for both EL and PL. In the first tests there was no obvious systematic variation of the spectra, as might be expected if one of the peaks that composes the broad defect band centered at 1.35 eV were associated with Cu. Grecu et al. [3] assigned this feature in PL to a Donor – Cu_{Cd} complex, while cathodoluminesence studies assign features in this area to Cu-vacancy acceptor complex with multiple donor states [4]. Further study of the spatial variation of spectra could prove very useful as it would allow for defect type and spatial identification.

Gas Jet / Vapor Transport Deposition

As reported previously the APCVD system, developed jointly with ITN Energy Systems under NREL contract ZAK-8-17619-03, suffered from low deposition rates or dust formation. This was subsequently replaced by a system initially named Jet Vapor Deposition (JVD), with deposition rates as high as 20 μm/minute. Interest in this system was spurred by the similarities to the processes used by NREL (Close Space Sublimation – CSS) and by First Solar (Vapor Transport Deposition – VTD). The fundamental difference between CSS and these other deposition methods is that in CSS mass transport occurs only by diffusion, while in the others transport is controlled by convection, which separates the source and substrate process variables. The name Gas Jet Deposition (GJD) was recently adopted to recognize the difference between the calculated gas velocities used and the sonic velocities characteristic of the patented JVD process.

A number of observations were made in this quarter regarding deposition. Details are available in Ref. 5.

- Deposition rates exceeded 20 μm/minute, approaching the high rates observed at First Solar. Growth rate was limited only by the source heater element.
- The growth rate increased exponentially with source temperature, with an activation energy of 42 kcal/mol (consistent with the activation energy of CdTe sublimation), indicating first order kinetics.
- Below 400ºC, the growth rate was independent of substrate temperature. Above 400ºC the rate dropped exponentially with substrate temperature due to resublimation.
- Films deposited at substrate temperatures below 400ºC showed discrete, columnar-like grains. Above 400ºC the grains became denser and less columnar.
- Growth rate was found to be relatively insensitive to chamber pressure in the regime of 1-10 Torr since under these conditions growth was reaction limited.

In this quarter a detailed model was developed for CdTe deposition to capture the critical parameters needed to scale the technology and determine sensitivity of the process. The role of mass transport, surface reactions and source and substrate conditions were examined. A Langmuir formulation was developed to describe the surface reaction probability that was consistent with experimental observations of resublimation. A major implication of the modeling is that GJD operates in a pressure regime where growth rates are near their maximum. Decreasing pressure results in lower growth rates due to a lower sticking coefficient. At higher pressures maintaining the inlet mole fraction (increasing source temperature) becomes a problem, as is potential gas phase nucleation. From this analysis optimum pressure conditions

are predicted as a function of source temperature. These are shown in the figure below as well as current operation conditions for a variety of vapor transport techniques, some surmised from known deposition rates and operating conditions.

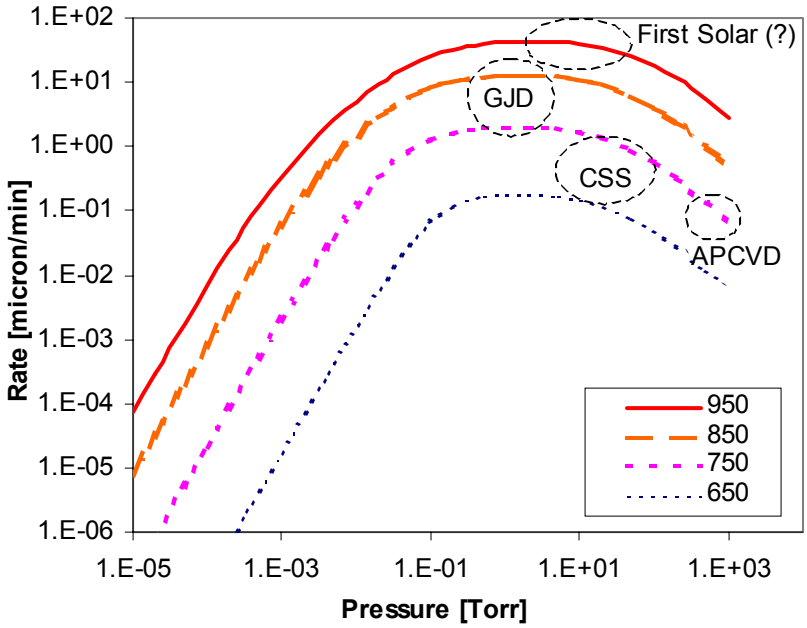

Figure 7 **Plot showing growth rates at operating regimes of various vapor transport deposition technologies. Legend indicates results for different source temperatures. For this model substrate temperature was held fixed at 500 ºC and He carrier flow rates of 150 sccm.**

Device optimization was another area of studies. We had previously reported results for CdS processing and substrate temperatures; results for $CdCl_2$ treatment, etching and back contact formation are described in Ref. 5. During this phase the use of high resistance buffer layers at the TCO/CdS interface was studied. Buffer layers have been shown to be responsible for increased open circuit voltage (V_{oc}) and fill factor (FF) as well as reproducibility in the cells [6]. The effect of highly resistive transparent (HRT) buffer layer thickness and resistivity were both evaluated. Undoped tin oxide films with thickness from 30 to 90 nm and resistivities 0.1 - 10 Ω-cm were deposited on commercial TCO by plasma enhanced chemical vapor deposition at CSM [7]. Cells were then made using thinner CdS films (140 nm vs. 290 nm).

The results of the average efficiency of the top 20 cells are plotted against buffer layer resistivity and thickness in Figure 8. Note that device data for a non-HRT sample is included in both figures for comparison. The CdTe deposition and post-processing for these samples were not ideal, resulting in some poor cells. It was difficult to ascertain any trends in device performance relative to HRT thickness or resistivity due to the limited data. Thinning the CdS layer showed no apparent increase in J_{sc}. Inclusion of the HRT buffer layers and thinner CdS also decreased V_{oc}. Average device efficiency with the HRT was due to an increase in FF that offset the loss in V_{oc}. One last interesting result was that EL images (not shown) of the cells with HRT layers were more uniform than those without. Further work will be required to determine whether these results are due to thinner CdS or the addition of the HRT layer, or both.

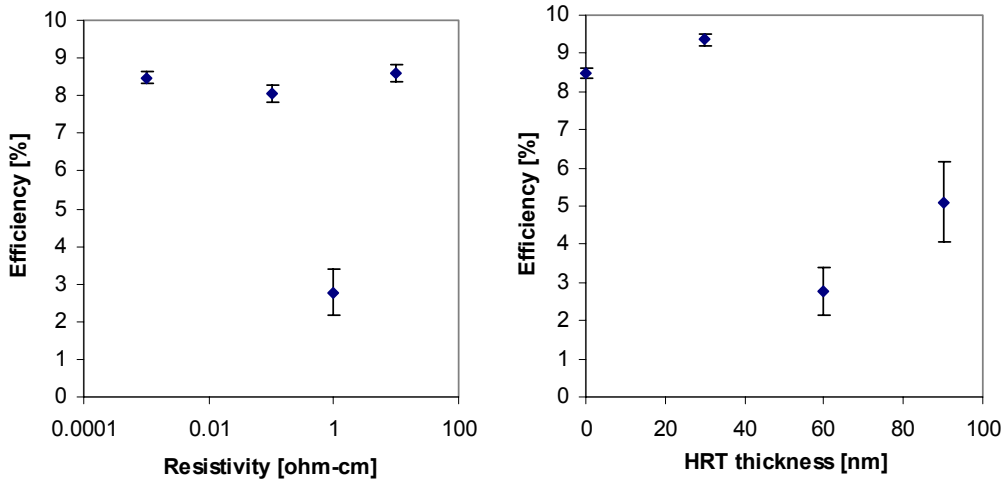

Figure 8 **Device efficiency plotted against HRT buffer layer resistivity (left, all HRT films nominally 60 nm thick) and thickness (right, all films nominally 1 Ω-cm). Data points at 0.001 Ω-cm (left) and 0 nm (right) represent devices made without a buffer layer.**

References

[1] V. G. Karpov, A. D. Compaan, and Diana Shvydka, Effects of nonuniformity in thin-film photovoltaics, Appl. Phys. Lett. 80, 4256 (2002).

[2] Diana Shvydka, J.P. Rakotoniaina and O. Breitenstein, Thermography Mapping and Modeling, CdTe team meeting, July 2003.

[3] D. Grecu, A. D. Compaan, D. Young, U. Jayamaha and D. H. Rose, Photoluminescence of Cu-doped CdTe and related stability issues in CdS/CdTe solar cells, J. Appl. Phys. 88, 2490 (2000); and D. Grecu and A. D. Compaan, Photoluminescence study of Cu diffusion and electromigration in CdTe, Appl. Phys. Lett. 75, 361 (1999).

[4] T.Gessert, M.J. Romero, M. J., S. Johnston, B. Keyes, P. Dippo, Spectroscopic Cathodoluminescence Studies of the ZnTe:Cu Contact Process for CdS/CdTe Solar Cells: Preprint. 7 pp.; NREL Report No CP-520-31438 (2002).

[5] J. Kestner, Development and Analysis of Vapor Transport Deposition of CdTe Thin Films, Ph.D. Thesis Chemical Engineering. 2003, Colorado School of Mines: Golden, CO.

[6] X. Wu, R. Ribelin, R.G. Dhere, D. Albin, T.A. Gessert, S. Asher, D.H. Levi, A. Mason, H.R. Moutinho, P. Sheldon, High-Efficiency $Cd_2SnO_4/Zn_2SnO_4/Zn_xCd_{1-x}S$/CdS/CdTe Polycrystalline Thin-Film Solar Cells. 28th IEEE Photovoltaic Specialists Conference 2000, Anchorage, Alaska. Institute of Electrical and Electronics Engineers, Inc.; pp. 470-474; NREL Report No. CP-520-28934 (2000). and X. Li, R. Ribelin, Y. Mahathongdy, D. Albin, R. Dhere, D. Rose, S. Asher, H. Moutinho, and P. Sheldon, Effect of High-Resistance SnO2 on CdS/CdTe Device Performance. NCPV Photovoltaics Program Review: Proceedings of the 15th Conference, 1998, Denver, Colorado. AIP Conference Proceedings 462. Woodbury, NY: AIP; pp. 230-235; NREL Report No. 27391 (1999).

[7] J. Robbins, Plasma enhanced chemical vapor deposition and physical characterization of tin oxide thin films, Masters Thesis, Chemical Engineering. 2000, Colorado School of Mines: Golden, CO.